Magna Scientia Advanced Biology and Pharmacy

eISSN: 2582-8363

Cross Ref DOI: 10.30574/msabp

Journal homepage: https://magnascientiapub.com/journals/msabp/

(RESEARCH ARTICLE)

In silico identification of approved drugs for potential prophylactic uses against SARS-CoV-2 infection

Roselyn N. Egbuna [1, 2, *], InnocentMary I. Ejiofor [3], Emmanuel C. Oranu [4], Ifeanyichukwu R. Iroha [5] and Ikemefuna C. Uzochukwu [6]

[1] *Department of Pharmaceutical Microbiology and Biotechnology, Faculty of Pharmaceutical Sciences, Chukwuemeka Odumegwu Ojukwu University, Igbariam, Anambra State, Nigeria.*
[2] *Department of Pharmaceutical Microbiology and Biotechnology, Faculty of Pharmaceutical Sciences, Nnamdi Azikiwe University, Agulu Campus, Anambra State, Nigeria.*
[3] *Department of Pharmacognosy and Traditional Medicine, Faculty of Pharmaceutical Sciences, Nnamdi Azikiwe University, Agulu Campus, Anambra State, Nigeria.*
[4] *Department of Pharmaceutical and Medicinal Chemistry, Faculty of Pharmaceutical Sciences, Chukwuemeka Odumegwu Ojukwu University, Igbariam, Anambra State, Nigeria.*
[5] *Department of Applied Microbiology, Faculty of Sciences, Ebonyi State University, Abakaliki, Nigeria.*
[6] *Department of Pharmaceutical and Medicinal Chemistry, Faculty of Pharmaceutical Sciences, Nnamdi Azikiwe University, Agulu Campus, Anambra State, Nigeria.*

Magna Scientia Advanced Biology and Pharmacy, 2024, 11(02), 057–071

Publication history: Received on 26 February 2024; revised on 08 April 2024; accepted on 10 April 2024

Article DOI: https://doi.org/10.30574/msabp.2024.11.2.0023

Abstract

The outbreak of Severe Acute Respiratory Syndrome Corona Virus (SARS-CoV-2) responsible for Coronavirus disease 2019 (COVID-19) constitute a major public health threat and economic burden. Despite the multifold research all over the world. COVID-19 has remained without a treatment. Hence, the urgent need to repurpose the FDA-approved drugs through *in silico* computational technique to identify inhibitors of SARS-CoV-2. Bioinformatics techniques were used to screen 2015 FDA- approved drugs against SARS-CoV-2 proteins and associated human protein, angiotensin-converting enzyme 2 (ACE2) to identify drug for new indication. The ligands were downloaded from Selleckchem drug data bank in SDF format. Open Babel was used to separate the ligands into their compounds and prepared for docking simulation using shell script and saved as PDBQT. Experimental crystal structures of the receptors (ACE2 and Spike proteins) were retrieved from Protein Data Bank (PDB), Autodock tools was used to prepare the proteins and saved as PDBQT files. Docking protocols were validated, molecular docking simulations were performed on a Linux platform using AutoDock Vina in quadruplicate. The binding energies (BEs) kcal/mol were calculated and expressed as mean ± standard deviation. Discovery studio was used for visualization. Density Functional Theory (DFT) was used to determine the predictive maximal inhibitory concentration (pIC_{50}) of best hits. Ninety-one (91) new hits were identified for prophylaxis. Four (4) compounds were subjected to DFT based IC_{50} calculation with molnupiravir as a reference compound. Significantly, calculated IC_{50} of molnupiravir in Vero cells and Calu-3 were 0.299 and 0.008µM respectively while the experimental IC_{50} in Vero cells and Calu-3 as reported in literature were 0.3 and 0.08 µM respectively. The newly identified hits are promising therapeutic agents and there is no significant difference between the experimental IC_{50} of molnupiravir and the calculated IC_{50}.

Keywords: SARS-CoV-2; Prophylaxis; *In silico*; Approved Drugs; DFT; IC_{50}

* Corresponding author: Roselyn N. Egbuna

1. Introduction

Outbreak of different pneumonia cases were recorded in Wuhan city, Province of Hubei, China by the end of 2019. The causative agent was identified as a novel coronavirus, named 2019-nCov. Coronavirus belong to the group of viruses infecting many different animals, and they are capable of causing mild to severe respiratory infections in human. World Health Organization (WHO) characterized coronavirus disease 2019 (COVID-19) as a pandemic on the 11th day of March 2020.

At the same time, The International Committee on Taxonomy of Viruses (ICTV) renamed the virus 2019-nCov to Severe Acute Respiratory Syndrome Coronavirus 2 (SARS-CoV-2), based on the genome sequencing analysis of the novel coronavirus and the disease as COVID-19 [1-3]. SARS-CoV-2 pathogen has infected over seven hundred and seventy-two million (precisely 772,138,818) globally and caused over six million (precisely 6,985,964) deaths as of 6:59pm CET, 6 December 2023 [4].

In Nigeria, from January 2020 to December 2023, there have been two hundred and sixty-seven thousand, one hundred and sixty-three (267,163) confirmed cases of COVID-19 with three thousand one hundred and fifty-five (3,155) deaths [4]. As a matter of urgency, there is a need to identify drugs for the treatment of COVID-19, so as to reduce mortality or morbidity. Though, several safety measures which include "stay at home" "work from home" "wearing of nose mask" "safe social distancing" "border closure" "lock down" etc. implemented in many countries for 2-3 months or more aided in flattening the curve but therapeutic measures are greatly needed.

Since the outbreak of COVID-19, there has been an increasing interest in finding a potential therapeutic agent for COVID-19. Molecular docking is a promising tool for drug discovery and development through the interaction of ligand (drug) molecules inside the binding pocket of a target protein (receptor) [5]. It offers the opportunity to study factors such as the identification of hit molecules, optimization of lead compounds and virtual screening [6-9].

In the present study, we utilized an *in silico* ligand-receptor binding modeling and performed a comprehensive virtual screening of two thousand and fifteen (2015) FDA-approved drugs, taking into cognizance list of already repurposed drugs against SARS-CoV-2 and calculated the predictive half maximal inhibitory concentration (IC_{50}) of the identified inhibitors through computational approach, density functional theory using molnupiravir as reference compound.

2. Materials and methods

Materials used and their sources include: personal computer HP 290 GIMT, Drug Bank database (https://www.selleckchem.com/h), Protein Data bank (PDB): RCSB PDB (www.rcsb.org), PubChem (http://pubchem.ncbi.nlm.gov), Data Warrior software, PyMol 2.5.4, Linux operating system (Ubuntu desktop 20.04 LTS), Windows operating system (Ubuntu 20.04 LTS), Open babel, BIOVIA Discovery Studio 2020, Microsoft office 2010, Autodock tools 1.5.6, AutoDockVina 11.2 on Ubuntu operating system, Maestro Schrödinger 11.0, Density Functional Theory (DFT), ORCA version 5.0.4, Avogadro-1.2.

2.1. Preparations of small molecules (ligands) approved drugs

The electronic structures of FDA approved drugs were obtained in SDF format from Selleckchem Inc. (Houston, TX, https://www.selleckchem.com) Drug Bank database [10]. The file was separated into their compounds using Open Babel [11] and prepared for docking simulations using shell script as reported elsewhere [12]. The script utilized obminimize [11] and General Amber Force Field (GAFF), which have parameters for most organic and pharmaceutical molecules [13]. Again, a total of the 2015 approved drugs were subjected to 2500 steps of geometry optimization using the steepest descent algorithm before generating the Protein Data Bank, Partial Charge (Q), and Atom Type (T) (PDBQT) file format for docking simulation studies.

2.2. Preparations of drug targets (receptors)

The protein structures used in the docking experiments were retrieved from the Research Collaboratory for Structural Bioinformatics Protein Data Bank (PDB). SARS-CoV-2 protein (spike glycoprotein) and human protein (ACE2) were used for the study. Their 3D atomic coordinates were obtained from Protein Data Bank (spike glycoprotein (PDB ID: 6VSB) human receptor, ACE2 (PDB ID: 1R4L) and prepared for molecular docking simulations. Briefly, duplicate chains, heteromolecules and water molecules were deleted, and polar hydrogen were added using PyMol and Autodock tools before generating the PDBQT files of the drug targets.

2.3. Grid map determination

The grid box sizes and centers (Table 1) at grid space of 1.0 Å and 8 exhaustiveness were generated and used for the docking simulations/virtual screening studies.

Table 1 Grid box sizes and centers at grid space of 1.0 Å and 8 exhaustiveness

Drug target	Size			Center		
	X	Y	Z	X	Y	Z
Spike glycoprotein (6VSB)	15	15	20	211.077	188.213	279.09
Human Angiotensin Converting Enzyme 2, ACE2 (1R4L)	18	15	18	40.913	5.106	27.505

2.4. Validations of Molecular Docking Protocols

To substantiate the anti-SARS-CoV-2 activity/host directed anti-SARS-CoV-2 prediction of our model/method, validation of molecular docking simulations protocols was carried out first. To this end, the experimental crystal complex of the human receptor, angiotensin converting enzyme 2 with (S,S)-2-{1-carboxy-2-[3-(3,5-dichloro-benzyl)-3H-Imidazol-4-yl]-ethylamino}-4-methyl-pentanoic acid was reproduced *in silico* and re-docked into the binding sites with AutoDockVina [14] using the grid box sizes and centers presented in Table 1. The binding energies and docked poses of the compounds to the drug target was calculated/visualized and compared with the experimental crystal complex. Also, blind docking of remdesivir into the SARS-CoV-2, spike glycoprotein (6VSB) was first performed and subsequently validated using grid box sizes and centers (Table 1.0).

2.5. Virtual Screening/Molecular Docking Simulations

All of the docking experiments were performed using AutoDock Vina (O. Trott, The Scripps Research Institute, La Jolla, CA, USA) as: (a) it offers more accuracy in predicting ligand-protein interactions than the previous version, AutoDock 4.2, (b) it offers a shorter running time as a result of multiple core processors, and (c) it offers greater accuracy for ligands with more than 20 rotatable bonds. All the approved drugs (2015) prepared in PDBQT file format were docked into the SARS-CoV-2 spike glycoprotein (6VSB), and human angiotensin converting enzyme 2, ACE2 (1R4L) using AutoDockVina [14] and after the validations of the molecular docking protocols or blind docking and re-docking simulations. The simulations were performed locally on a Linux platform using a configuration file and script containing information on the grid box centers and sizes of prepared receptors (spike glycoprotein, and human angiotensin converting enzyme 2). The binding energies (BEs) (kcal/mol) (n = 4) from the molecular docking simulations were calculated and expressed as mean ± standard deviation. The approved drugs with better binding energies for the receptor than the reference compounds ((S,S)-2-{1-carboxy-2-[3-(3,5-dichloro-benzyl)-3H-Imidazol-4-yl]-ethylamino}-4-methyl-pentanoic acid and remdesivir) were identified, profiled for possible prophylactic uses against SARS-CoV-2. Also, their binding poses were visualized with Discovery Studio and compared with the reference compounds.

2.6. Post Docking Analysis

After the molecular docking simulation, the binding energies from the molecular docking simulations and average inhibition constants (Ki) were calculated and expressed as mean ± standard deviation using Microsoft Excel. The binding poses of front runners were visualized using PyMol and Discovery Studio.

2.6.1. Multi-target drug for prophylaxis

Drugs identified for possible prophylactic use were selected based on their interactions with the SARS-CoV-2 spike glycoproteins (6VSB) and angiotensin-converting enzyme -2 (1R4L). This is because SARS-CoV-2 trimeric spike (S) glycoprotein interact with the human ACE2 receptor to mediate viral entry into host cells [15-18]. Again, ACE2 is not expressed in the respiratory system only but also in the kidneys and gastrointestinal tract, subjecting these organs to SARS-CoV-2 invasion [19-21].

2.7. Relative Half maximal inhibitory concentration (IC_{50})

The 3-dimensional structures of the ligands (celecoxib, indinavir, raltegravir, itraconazole and molnupiravir) were obtained from PubChem [22]. All calculations were performed using the Orca (version 5.0.4) after generating the input files with Avogadro-1.2. The optimizations of the ground-state geometries of the ligands were performed with B3LYP

functional and the 6-31G (d, p) basis set [23-27]. Analytical vibrational frequency calculations (at the same level of theory) were subsequently carried out until convergence to the true minima (no imaginary frequencies) [28]. The electric dipole moments and reactivity descriptors such as absolute hardness (η), absolute electronegativity (χ) and reactivity index (ω) of the ligands were computed with equations 1 to 3 [29] and after DFT calculations at the same level of theory and basis set.

$$\eta = \frac{E_{LUMO} - E_{HOMO}}{2} \quad \ldots\ldots 1$$

$$\chi = \frac{E_{LUMO} + E_{HOMO}}{2} \quad \ldots\ldots 2$$

$$\omega = \frac{\chi^2}{2\eta} \quad \ldots\ldots 3$$

where E_{HOMO} is the highest occupied molecular orbital energy and E_{LUMO} is the lowest unoccupied molecular orbital energy. The electric dipole moments and the calculated reactivity descriptors were used for calculation of the relative IC50 according to equation 4 reported elsewhere [24].

$$(IC_{50})_{lig} = (IC_{50})_{ref} \frac{W_{lig}}{W_{ref}} e^{(\mu_{ref} - \mu_{lig})} \quad \ldots\ldots 4$$

where μ_{lig} and μ_{ref} are the electric dipole moment of the ligands and reference respectively while W_{lig} and W_{ref} are the reactivity descriptors of the ligands and reference respectively.

3. Results

3.1. Validation of Docking Protocols

In order to validate and check the efficiency of the docking procedure, a re-docking of the co-crystallized ligand was performed. The superposition between the co-crystallized ligand and the docked ligand conformation was displayed in Figure 1. Blue sticks represents the co-crystallized ligand while the Green and Red sticks represents the docked ligands. The docking protocols defines the binding pockets of each of the receptors, and these outcomes reveals that molecular docking simulation was effectively verified.

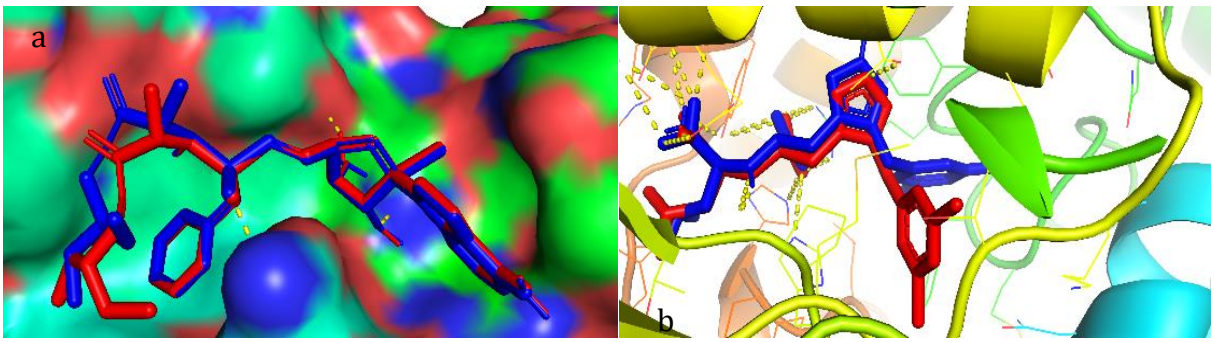

Figure 1 Validation of docking protocols for virtual screening. (a) 6VSB - Spike Glycoprotein, (b) IR4L- Human receptor, angiotensin-converting enzyme 2 (ACE2)

3.2. Drugs identified for prophylaxis

SARS-CoV-2 proteins targeted for identifying drugs for prophylactic usage were spike glycoproteins (6VSB) and associated human drug target, Angiotensin-converting enzyme 2, ACE2 (1R4L). Ninety-one (91) drugs were identified as possible inhibitors of SARS-CoV-2 spike glycoproteins from attaching to Angiotensin-converting enzyme 2 as they have good binding energies (Table 2.0). Also, atazanavir, boceprevir, indinavir, lopinavir, nelfinavir, raltegravir and ritonavir already reported in literature to have inhibitory activity against SARS-CoV-2 are evidenced here in. Significantly, celecoxib and dustasteride which happen to be an NSAID used for the management of rheumatoid arthritis and benign prostrate hyperplasia (BPH) respectively had better binding energies and were picked as the representative of the ninety-one (91) drugs identified for prophylaxis. Molecular interactions of these representatives are shown in

Table 2 Binding energies and previous indication of drugs identified for potential prophylactic use against SARS-CoV-2 infection

S/N	Drugs	6VSB	1R4L	Previous indication
1	Alprazolam	-6.6±0.00	-9.2±0.00	A triazolobenzodiazepine used to treat panic disorders and generalized anxiety in addition to anxiety associated with depression.
2	Artesunate	-6.9±0.00	-9.3±0.00	An artemesinin derivative indicated for the treatment of severe malaria.
3	*Atazanavir[(a)]	-7.1±0.00	-10.4±0.00	An antiviral protease inhibitor used in combination with other antiretrovirals for the treatment of HIV.
4	Atovaquone	-7.4±0.00	-10.4±0.00	An antimicrobial indicated for the prevention and treatment of *Pneumocystis jirovecii* pneumonia (PCP) and for the prevention and treatment of Plasmodium falciparum malaria.
5	Benazepril	-6.5±0.00	-9.3±0.15	An ACE inhibitor prodrug used to treat hypertension.
6	Benzylpenicillin	-6.6±0.00	-8.925±0.04	An antibiotic.
7	*Boceprevir[(a)]	-6.7±0.00	-10.4±0.00	A hepatitis C virus NS3/4A protease inhibitor used in combination with other medications to treat chronic hepatitis C genotype 1 infection.
8	Bromocriptine	-7.5±0.00	-8.8±0.00	A dopamine D2 receptor agonist used for the treatment of prolactin-related conditions, as well as in early Parkinsonian Syndrome.
9	Carbamazepine	-6.7±0.00	-8. 7±0.00	An anticonvulsant used to treat various types of seizures and pain resulting from trigeminal neuralgia.
10	Cefaclor	-7.3±0.00	-9.6±0.00	A second-generation cephalosporin (antibiotic).
11	Cefadroxil	-6.7±0.00	-9.8±0.00	A cephalosporin antibiotic.
12	Cefalotin	-6.5±0.00	-9.025±0.04	A broad-spectrum cephalosporin antibiotic.
13	Cefazolin	-6.7±0.00	-9.55±0.08	A broad-spectrum cephalosporin antibiotic.
14	Ceftazidime	-7±0.00	-9.4±0.00	A broad-spectrum third-generation cephalosporin beta-lactam antibiotic.
15	Ceftriaxone	-7.2±0.00	-9±0.00	A broad-spectrum cephalosporin antibiotic.
16	Cefuroxime	-6.6±0.00	-9.2±0.00	A cephalosporin antibiotic.
17	Celecoxib	-7.2±0.00	-9.7±0.00	An NSAID used to treat osteoarthritis, rheumatoid arthritis, acute pain, menstrual symptoms, and to reduce polyps is familial adenomatous polyposis.
18	Cephalexin	-6.6±0.00	-9.4±0.00	A first-generation cephalosporin (antibiotic).
19	Chlorhexidine	-7.1±0.00	-8.675±0.19	An antiseptic used to sterilize for surgeries.

20	Cinnarizine	-7.1±0.00	-10.375±0.04	Used for the management of labyrinthine disorder symptoms, including vertigo, tinnitus, nystagmus, nausea, and vomiting.
21	Clomifene	-6.7±0.00	-9.175±0.04	Used mainly in female infertility due to anovulation (e.g. due to polycystic ovary syndrome) to induce ovulation.
22	Clonazepam	-6.8±0.00	-8.9±0.00	A long-acting benzodiazepine used to treat panic disorders, severe anxiety, and seizures.
23	Cloxacillin	-6.9±0.00	-10.4±0.00	An antibiotic.
24	Cloxazolam	-6.5±0.00	-9.8±0.00	Used primarily as an anti-anxiety agent.
25	Clozapine	-6.5±0.00	-9.6±0.00	An antipsychotic drug used in treatment resistant schizophrenia.
26	Cyproheptadine	-7±0.00	-9.5±0.00	Combined serotonin and histamine antagonist used in the treatment of allergic symptoms, for appetite stimulation, and off-label in the treatment of serotonin syndrome.
27	Danazol	-6.6±0.00	-9.6±0.00	Used for the treatment of endometriosis and fibrocystic breast disease
28	Deslanoside	-8.8±0.00	-9.825±0.26	Used for the treatment and management of Congestive cardiac insufficiency, arrhythmias and heart failure.
29	Dexamethasone	-6.5±0.00	-8.8±0.00	A glucocorticoid used for the treatment of various inflammatory conditions, including bronchial asthma, as well as endocrine and rheumatic disorders.
30	Diosmin	-7.3±0.00	-10.8±0.00	Used to support vein and capillary function.
31	Domperidone	-7.3±0.00	-9.4±0.00	A dopamine receptor antagonist used as a peristaltic stimulant and anti-emetic agent for dyspepsia, indigestion, epigastric pain, nausea, and vomiting.
32	Donepezil	-7.2±0.00	-9.3±0.00	An acetylcholinesterase inhibitor used to treat the behavioral and cognitive effects of Alzheimer's Disease and other types of dementia.
33	Doxazosin	-6.9±0.00	-11±0.00	Indicated to treat the symptoms of benign prostatic hypertrophy.
34	Dutasteride	-9.1±0.00	-10.675±0.11	An antiandrogenic compound that is used for the treatment of symptomatic benign prostatic hyperplasia (BPH).
35	Ergotamine	-8.1±0.00	-11.1±0.00	Therapy to abort or prevent vascular headache, e.g., migraine.
36	Flubendazole	-7.2±0.00	-9.5±0.00	An anthelmintic that is used to treat worm infection in humans. It is available OTC in Europe.
37	Flucloxacillin	-7.2±0.00	-9.9±0.00	A narrow-spectrum penicillin antibiotic.
38	Flunarizine	-7.3±0.00	-10.525±0.11	A selective calcium-entry blocker used as migraine prophylaxis in patients with severe and frequent episodes who have not responded adequately to more common treatments

39	Flunitrazepam	-6.6±0.00	-8.9±0.00	Benzodiazepine used to manage anxiety disorders and insomnia.
40	Folic Acid	-7.6±0.00	-10.2±0.00	Nutrient used to treat megaloblastic anemia.
41	Gemifloxacin	-6.5±0.00	-9.1±0.00	A quinolone antibacterial agent.
42	Gliclazide	-6.6±0.00	-9.2±0.00	A sulfonylurea drug used to treat hyperglycemia in patients with type 2 diabetes mellitus.
43	Glimepiride	-7.5±0.00	-10.1±0.00	A sulfonylurea drug used to treat type 2 diabetes mellitus.
44	Glyburide	-7.8±0.00	-10.75±0.08	A sulfonylurea used in the treatment of non-insulin dependent diabetes mellitus.
45	Haloperidol	-7±0.00	-9.3±0.00	An antipsychotic agent used to treat schizophrenia and other psychoses.
46	Hesperetin	-6.7±0.00	-8.8±0.00	Used for lowering cholesterol and, possibly, otherwise favorably affecting lipids.
47	Indapamide	-6.8±0.00	-8.9±0.00	A thiazide diuretic used to treat hypertension as well as edema due to congestive heart failure.
48	*Indinavir[(a)]	-7.6±0.00	-9.975±0.19	A protease inhibitor used to treat HIV infection
49	Irbesartan	-8.3±0.00	-10±0.00	An angiotensin receptor blocker used to treat hypertension and treat congestive heart failure.
50	Itraconazole	-7.4±0.00	-11.5±0.00	An anti-fungal agent.
51	Ketoconazole	-7.9±0.00	-10.275±0.11	A broad-spectrum antifungal used to treat seborrheic dermatitis and fungal skin infections.
52	Lansoprazole	-6.7±0.00	-9.2±0.00	A proton pump inhibitor used to help gastrointestinal ulcers heal, to treat symptoms of gastroesophageal reflux disease (GERD.
53	Loperamide	-7.3±0.00	-10.9±0.00	Used for the control and symptomatic relief of acute nonspecific diarrhea and of chronic diarrhea associated with inflammatory bowel disease or gastroenteritis.
54	*Lopinavir[(a)]	-7.3±0.00	-11.05±0.08	Indicated for the treatment of human immunodeficiency virus (HIV) infection
55	Loratadine	-6.8±0.00	-9.7±0.00	A second-generation antihistamine used to manage the symptoms of allergic rhinitis.
56	Lorazepam	-6.6±0.00	-9±0.00	A short-acting benzodiazepine commonly used to treat panic disorders, severe anxiety, and seizures.
57	Losartan	-7.8±0.00	-9.2±0.00	An angiotensin receptor blocker used to treat hypertension and diabetic nephropathy and is used to reduce the risk of stroke.
58	Mebendazole	-7±0.00	-9.5±0.00	A benzimidazole anthelmintic used to treat helminth infections.
59	Mefloquine	-6.7±0.00	-9±0.00	Antimalarial agent used in the prophylaxis and treatment of malaria.
60	Mifepristone	-7.7±0.00	-9.35±0.00	A cortisol receptor blocker used to treat Cushing's syndrome, and to terminate pregnancies up to 70 days gestation.

61	Minocycline	-6.7±0.00	-9±0.00	A tetracycline analog used to treat a wide variety of infections in the body.
62	Montelukast	-8.2±0.00	-10.625±0.11	A leukotriene receptor antagonist used as part of an asthma therapy regimen.
63	Morphine	-7.6±0.00	-9.1±0.00	An opioid agonist used for the relief of moderate to severe acute and chronic pain
64	Naloxone	-6.5±0.00	-8.7±0.00	An opioid receptor antagonist used to rapidly reverse an opioid overdose.
65	*Nelfinavir[a]	-7±0.00	-10.275±0.19	A viral protease inhibitor used in the treatment of HIV infection.
66	Novobiocin	-8.3±0.00	-11.475±0.04	An antibiotic used for the treatment of infections due to staphylococci.
67	Olmesartan	-7.6±0.00	-10.2±0.00	An angiotensin receptor blocker (ARB) used in the treatment of hypertension.
68	Ondansetron	-6.7±0.00	-8.7±0.00	A serotonin 5-HT3 receptor antagonist used to prevent nausea and vomiting in cancer chemotherapy and postoperatively.
69	Oxacillin	-7.2±0.00	-10.075±0.04	Used in the treatment of resistant staphylococci infections.
70	Oxytetracycline	-6.8±0.00	-10±0.00	A tetracycline antibiotic used to treat a wide variety of susceptible bacterial infections.
71	Pioglitazone	-7±0.00	-9.375±0.04	A thiazolidinedione used adjunctively with diet and exercise to normalize glycemic levels in adults with type 2 diabetes mellitus.
72	Piroxicam	-7±0.00	-9.475±0.04	An NSAID used to treat the symptoms of osteoarthritis and rheumatoid arthritis.
73	Praziquantel	-6.5±0.00	-9.3±0.00	An anthelmintic medication used to treat several parasitic worm infections such as schistosomiasis.
74	*Raltegravir[a]	-8.1±0.00	-10.1±0.00	An antiretroviral agent used for the treatment of HIV infections in conjunction with other antiretrovirals.
75	Ramipril	-6.6±0.00	-8.925±0.04	An ACE inhibitor used for the management of hypertension and the reduction of cardiovascular mortality.
76	Repaglinide	-6.5±0.00	-9.9±0.00	An antihyperglycemic used to improve glycemic control in diabetes.
77	Reserpine	-7±0.00	-10.075±0.11	Indicated for the for the treatment of hypertension
78	*Ritonavir[a] [b]	-6.7±0.00	-10.775±0.04	A HIV protease inhibitor used in combination with other antivirals in the treatment of HIV infection.
79	Sildenafil	-7±0.00	-9.8±0.00	Phosphodiesterase inhibitor used for the treatment of erectile dysfunction.
80	Spironolactone	-6.6±0.00	-9.9±0.00	Aldosterone receptor antagonist used for the treatment of hypertension.
81	Tadalafil	-7.7±0.00	-11.2±0.00	Indicated for the treatment of erectile dysfunction (ED); treatment of pulmonary arterial hypertension (PAH)
82	Tasosartan	-8.425±0.04	-11.125±0.04	Indicated for the treatment of hypertension and heart failure.
83	Telmisartan	-8.7±0.00	-10.925±0.04	Used alone or in combination with other classes of antihypertensives for the treatment of hypertension.

84	Tenofovir alafenamide	-7±0.00	-9.075±0.04	A nucleoside analog reverse transcriptase inhibitor used for the treatment of chronic hepatitis B virus infection in adults with compensated liver disease.
85	Tenofovir disoproxil	-7.2±0.00	-9.525±0.26	A nucleotide analog reverse transcriptase inhibitor used in the treatment of Hepatitis B infection and used in the management of HIV-1 infection.
86	Terazosin	-6.7±0.00	-9.7±0.00	An alpha-1 adrenergic antagonist used in the treatment of symptomatic benign prostatic hyperplasia and management of hypertension.
87	Tetracycline	-6.8±0.00	-10.3±0.00	An antibiotic used to treat a wide variety of susceptible infections.
88	Valsartan	-7.6±0.00	-10.225±0.26	Indicated for the treatment of hypertension to reduce the risk of fatal and nonfatal cardiovascular events, primarily strokes and myocardial infarctions.
89	Yohimbine	-6.9±0.00	-9.375±0.04	Indicated as a sympatholytic and mydriatic. Impotence has been successfully treated with yohimbine in male patients with vascular or diabetic origins and psychogenic origins.
90	*Molnupirivir[b]	-6.28±0.04	-8.4±0.05	An orally bioavailable isopropylester cytidine analog used to treat COVID-19.
91	*Nirmatrelvir[b]	-6.15±0.10	-9.25±0.05	An oral protease inhibitor with emergency use authorization for the treatment of mild-to-moderate COVID-19.

Key: 6VSB - spike glycoprotein, IR4L- human receptor, angiotensin-converting enzyme 2 (ACE2),; *Drugs previously reported to have effect against SARS-CoV-2 which is evidenced in this study; [a]Drugs previously reported to have effect against SARS-CoV-2 which is identified in this study for prophylaxis.; [b]Drugs approved for COVID-19 treatment: paxlovid (nirmatrelvir and ritonavir) and molnupiravir

Figure 2 as against molnupiravir. Furthermore, molecular interactions of raltegravir and lopinavir which represent the drugs already reported in literature as evidenced in this study are shown in Figure 3. z

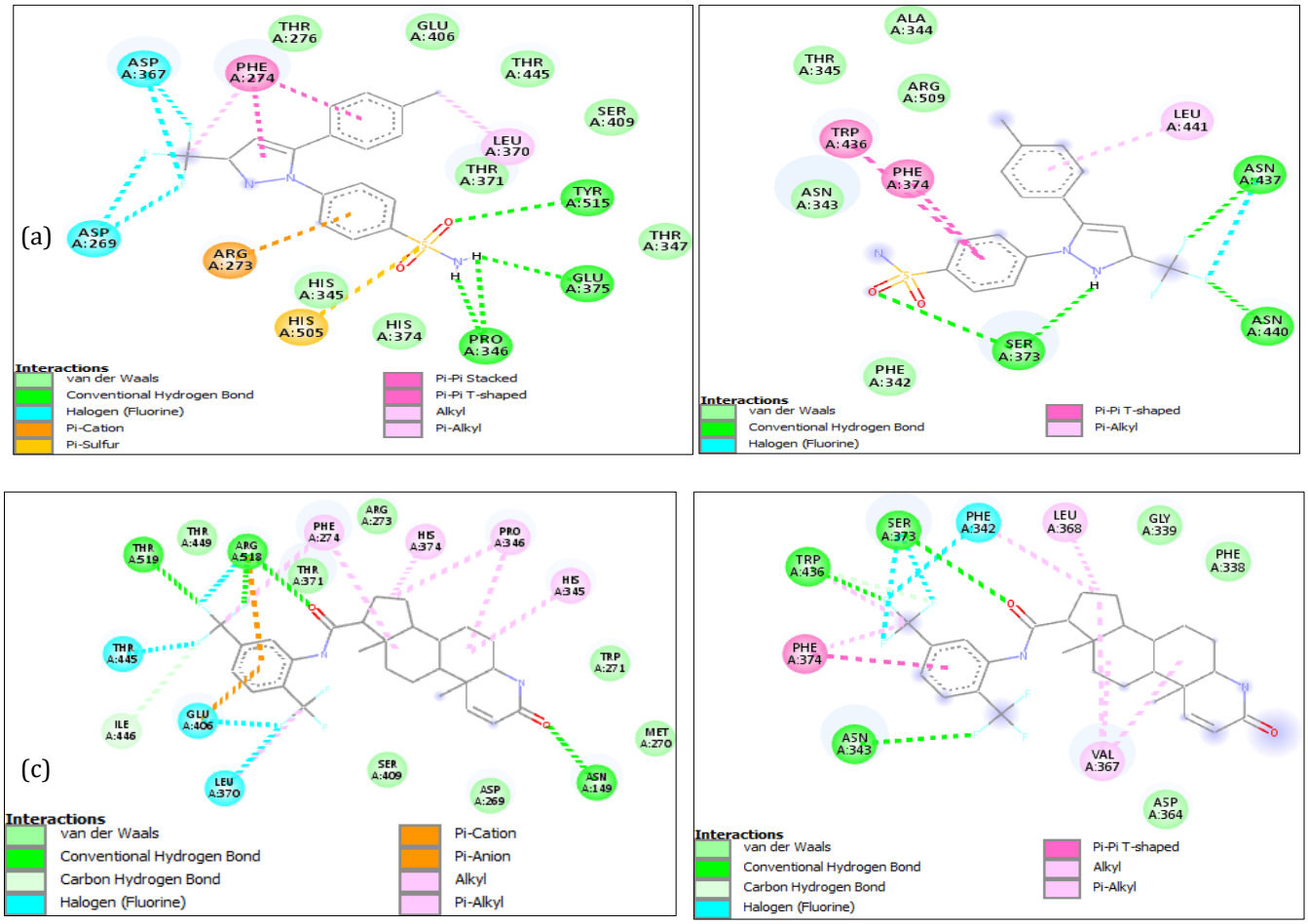

Figure 2 Molecular interaction between celecoxib, dutasteride and SARS-CoV-2 protein for prophylactic use.

(a) Celecoxib and SARS-CoV-2 IR4L-human receptor, angiotensin-converting enzyme 2 (ACE2), (b) Celecoxib and 6VSB-spike glycoprotein, (c) Dutasteride and IR4L, (d) Dutasteride and 6VSB-spike glycoprotein.

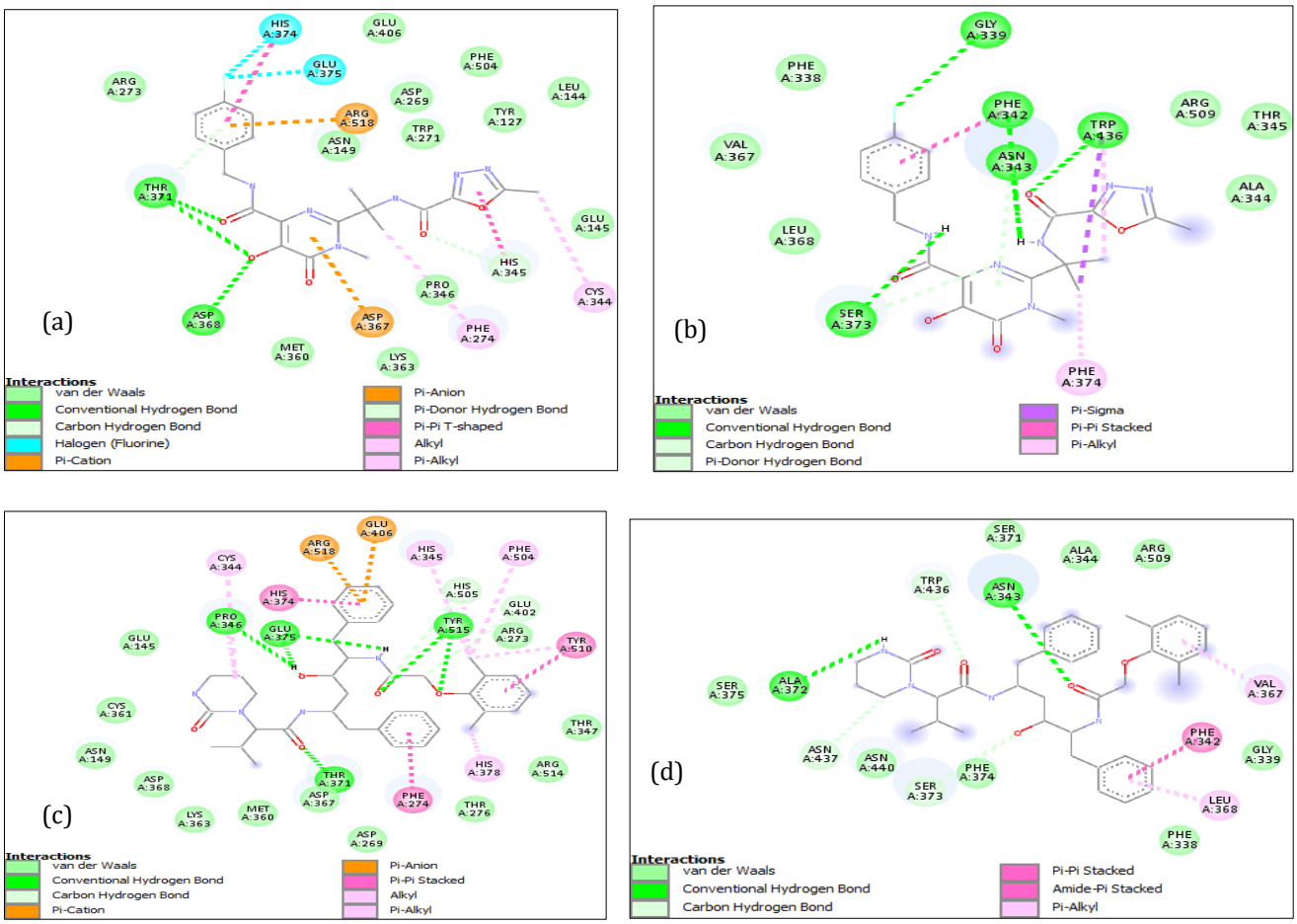

Figure 3 Molecular interaction between Raltegravir, Lopinavir and SARS-CoV-2 protein already reported in literature for prophylaxis.

(a) Raltegravir and SARS-CoV-2 IR4L-human receptor, angiotensin-converting enzyme 2 (ACE2), (b) Raltegravir and 6VSB-spike glycoprotein, (c) Lopinavir and IR4L, angiotensin-converting enzyme 2 (ACE2) (d) Lopinavir and 6VSB-spike glycoprotein

3.3. Quantum energetic parameters for prophylaxis

Quantum energetic parameters such as, dipole moment (μ), highest occupied molecular orbital (E_{HOMO}), lowest unoccupied molecular orbital (E_{LUMO}), energy difference or gap (ΔE) between E_{HOMO} and E_{LUMO}, electron affinity (A), and ionization potential (I) were calculated from the obtained optimized structure for celecoxib, indinavir, raltegravir, itraconazole as against molnupiravir, the reference drug for prophylactic use (Table 3).

Table 3 Energetic Parameters of Selected Compound for Prophylaxis

S/N	Drug name	Electric dipole (Debye)	E_{HOMO} (eV)	E_{LUMO} (eV)	Egap (eV)	I = -E_{HOMO} I (eV)	A = -E_{LUMO} A(eV)
1	Celecoxib	3.76928	-6.401	-1.517	-4.884	6.401	1.517
2	Indinavir	2.66886	-5.781	-0.549	-5.232	5.781	0.549
3	Raltegravir	7.17708	-6.232	-1.807	-4.425	6.232	1.807
4	Itraconazole	4.51016	-4.864	-0.932	-3.932	4.864	0.932
5	Molnupiravir	8.22423	-5.846	-0.867	-4.979	5.846	0.867

3.4. Quantum chemical descriptors and IC_{50} for prophylaxis

Quantum chemical descriptors/global parameters: absolute electronegativity (χ), absolute hardness (η), electrophilicity index (ω) and relative toxicity (γ) of celecoxib, indinavir, raltegravir, itraconazole as against molnupiravir, the reference drug for prophylactic use were calculated together with their respective IC_{50} (Table 4.0).

Table 4 Quantum Chemical Descriptors and IC_{50} of Selected Compound for Prophylaxis

S/N	Drug name	$\eta = E_{LUMO} - E_{HOMO}/2$	$x = E_{LUMO} + E_{HOMO}/2$	$\omega = x^2/2\eta$	IC_{50} Calu3	IC_{50} vero cells
1	Celecoxib	-2.442	3.959	-19.1375645	3.184091	11.94034131
2	Indinavir	-2.616	3.165	-13.1025303	0.014206	0.053272017
3	Raltegravir	-2.2125	4.0195	-17.87299565	1.280956	4.803584726
4	Itraconazole	-1.966	2.898	-8.255631132	0.000129	0.000482002
5	Molnupiravir	-2.4895	3.3565	-14.02346833	0.08	0.299999999

4. Discussion

COVID-19 pandemic caused by SARS-CoV-2 is a global threat. Scientists and physicians all over the world are searching for potential drugs for the treatment of COVID-19, and there is an urgent need to identify effective inhibitors of SARS-CoV-2 with lower side effects.

Drug repurposing represents a promising approach to recognize off-label indications for formerly approved drugs that are different from their conventional medical uses. This approach offers the advantage of minimizing the required time, cost, and efforts for drug discovery process and safety evaluation. From the findings of this study, celecoxib and dutasteride appears to have promising inhibitory effect on SARS-CoV-2 spike protein and associated human receptor, ACE2 compared to molnupiravir in the analysis above. Elsewhere, the drugs montelukast and celecoxib can cross blood brain barrier [30,31], which gives additional advantage to counter neurological manifestation of COVID-19. These drugs were reported to have appreciable inhibitory activity (IC_{50}) against SARS-CoV-2 [32]. Raltegravir and lopinavir already reported in literature appears to have more promising inhibitory effect on SARS-CoV-2 spike glycoprotein and ACE2 for prophylactic use than molnupiravir.

Among the eighty-nine selected drugs for prophylaxis, our results confirmed some of the suggested SARS-CoV-2 inhibitors in our study including remdesivir, raltegravir, lopinavir, ritonavir, atazanavir, boceprevir, indinavir nelfinavir, nirmatrelvir, saquinavir and simeprevir [33-36]. Few other drugs already approved for COVID-19 treatment though still undergoing clinical trial; molnupiravir and paxlovid (nirmatrelvir + ritonavir) are evidenced in this study. Remdesivir which is a nucleoside analog inhibitor of RNA polymerases with a large viral spectrum [37], this drug has been tested both *in vitro* and *in vivo* experiments (mice and Rhesus monkeys) against SARS-CoV-2 [38,39], indinavir an antiretroviral protease inhibitor used against type1 HIV infection.

Our computed IC_{50} for celecoxib in Calu3 and Vero cells are 3.184091 and 11.94034131μM, indinavir, 0.014206 and 0.053272017μM, raltegravir, 1.280956 and 4.803584726μM, itraconazole, 0.000129 and 0.000482002μM. The experimental IC_{50} of molnupiravir against SARS-CoV-2 as reported by Sheahan *et al*. [40] was 0.3μM in Vero cells and 0.08μM in human lung epithelial cell line Calu-3 while the calculated pIC_{50} of molnupiravir in this study is 0.299μM approximately 0.3μM in Vero cells and 0.08μM in Calu-3. Itraconazole showed the lowest IC50 value of 0.000129 and 0.000482002μM in Calu-3 and Vero cells respectively followed by indinavir, molnupiravir and raltegravir, while celecoxib has the highest IC_{50} value of 3.184091 and 11.94034131μM. Interestingly, Kumar *et al*. [32] reported that dose dependent IC_{50} of their I*n vitro* validation study of celecoxib amongst other drugs in Vero cells read 3.25μM with cytotoxicity (CC_{50}) >20μM which is in agreement with our computed IC_{50} for celecoxib.

Inference from this study, would be that molnupiravir though, still undergoing clinical trial is best fit for prophylactic use. Further investigation and validation study need to be carried out on these newly identified possible inhibitors of SARS-CoV-2. However, ninety-one (91) compounds identified for prophylaxis in this study had better binding energy with the two receptors used in this study, SARS-CoV-2 spike glycoprotein and human ACE2 receptor than the reference compound, molnupiravir. Suggesting that they may work mainly through other mechanism (e.g. Immunomodulation, or in combination with other compound in COVID-19 treatment.

5. Conclusion

SARS-CoV-2 infection is a life threatening disease with such a high transmission rate that can surpass even the most well-structured health systems in developed high-income countries. While more research is ongoing towards identifying therapeutic agents to combat this infectious disease, it is pertinent to consider the inhibitors identified in this study and exhaustively repurpose existing drugs as it has the advantage of exploiting molecules which have already been tested in terms of toxicity and which are usually easy to purchase for clinical tests and patient administration. Therefore, positive results from this kind of procedure can speed up the process of finding a treatment against SARS-CoV-2. However, the number of approved drugs by the major jurisdictions is huge and directly performing either *in vitro* or *in vivo* studies on all of them would be time-consuming; thus a fundamental contribution to accelerate the screening can come from *in silico* techniques. The compound identified herein has promising inhibitory properties against SARS-CoV-2 and should be considered for further investigation and possible management of COVID-19.

Compliance with ethical standards

Disclosure of conflict of interest

The authors declare no conflict of interest.

References

[1] Cui, J., Li, F., Shi, Z-L. (2019). Origin and Evolution of Pathogenic Coronaviruses. Nat. Rev. Microbiol. 17:181-192. https://doi.org/10.1038/s41579-018-0118-9

[2] Lai, C. C., Shih, T. P., Ko, W.C., Tang, H. J., Hsueh, P. R. (2020). Severe acute respiratory syndrome coronavirus 2 (SARS-CoV-2) and coronavirus disease-2019 (COVID-19): The epidemic and the challenges. Int J Antimicrob Agents. 55(3):105924. https://doi.org/10.1016/j.ijantimicag.2020.105924

[3] World Health Organization (WHO) (2020). Coronavirus disease (COVID-19) outbreak; https://www.who.int/emergencies/diseases/novel-coronavirus-2019.

[4] World Health Organization (WHO) (2023). WHO COVID-19 dashboard: COVID-19 cases. https://COVID-19.who.int/

[5] McConkey, B., Sobolev, V., Edelman, M. (2002). The performance of current methods in ligand-protein docking. Curr Sci;83(7) pp.845-856. http://www.jstor.org/stable/24107087.

[6] Jorgensen, W.L. (2004). The many roles of computation in drug discovery. Science 303:1813–8. https://doi.org/10.1126/science.1096361

[7] Bajorath, J. (2002). Integration of virtual and high-throughput screening. Nat Rev Drug Discov.1:882–894. https://doi.org/10.1038/nrd941

[8] Langer, T., Hoffmann, R.D. (2001). Virtual screening: an effective tool for lead structure discovery? Curr Pharm Des. 7:509–527. https://doi.org/10.2174/1381612013397861

[9] Kitchen, D.B., Decornez, H., Furr, J.R., Bajorath, J. (2004). Docking and scoring in virtual screening for drug discovery: methods and applications. Nat Rev Drug Discov. 3:935–949. https://doi.org/10.1038/nrd1549

[10] Wishart, D. S., Feunang, Y. D., Guo, A. C., Lo, E.J., Marcu, A., Grant, J.R., et al. (2018) Drug Bank 5.0: A Major Update to the DrugBank Database for 2018. Nucleic Acids Research, 4:(46) D1074-D1082. https://doi.org/10.1093/nar/gkx1037.

[11] O'Boyle, N.M., Banck, M., James, C.A., Morley, C., Vandermeersch, T., Hutchison, G. R. (2011). Open Babel: An Open Chemical Toolbox. J Cheminform. 3:33. https://doi.org/10.1186/1758-2946-3-33

[12] Ezeh, M.I., Okonkwo, O.E., Okpoli, I.N., Orji, C. E., Modozie, B.U., Onyema, A.C., Ezebuo, F.C. (2022). Cheminformatic Design and Profiling of Derivatives of Zika virus RNA-Dependent RNA polymerase and Methyltransferase. ACS Omega 7:33330 -33348. https://doi.org/10.1021/acsomega.2c03945

[13] Wang, J., Wolf, R. M., Caldwell, J.W., Kollman, P.A., Case, D.A. (2004). Development and testing of a general amber force field. J. Comput. Chem. 25: 1157-1174. https://doi.org/10.1002/jcc.20035

[14] Trott, O., Olson, A. J. (2009). AutoDock Vina: Improving the speed and accuracy of docking with a new scoring function, efficient optimization, and multithreading. J. Comput. Chem. 31, 455-461. https://doi.org/10.1002%2Fjcc.21334

[15] Cong Xu, Wang, Y. Liu, C., Zhang, C., Han, W., Hong, X. Wang, Y., et al. (2021). Conformational dynamics of SARS-CoV-2 trimeric spike glycoprotein in complex with receptor ACE2 revealed by cryo-EM. Sci. Adv. 1,7(1). https://doi.org/10.1126/sciadv.abe5575

[16] Basu, A., Sarkar, A., Maulik, U. (2020). Molecular docking study of potential phytochemicals and their effects on the complex of SARS-CoV2 spike protein and human ACE2. Scientific Reports, 10(1). https://doi.org/10.1038/s41598-020-74715-4

[17] Xu, X. Chen, P., Wang, J., Feng, J., Zhou, H., Li, X., Zhong, W., Hao, P.(2020). Evolution of the novel coronavirus from the ongoing Wuhan outbreak and modeling of its Spike protein for risk of human transmission. Sci. China Life Sci. 63(3): 457-460. https://doi.org/10.1007/s11427-020-1637-5

[18] Li, F., Li, W., Farzan, M., Harrison, S.C. (2005). Structure of SARS coronavirus spike receptor-binding domain complexed with receptor. Science. 309:1864–8. https://doi.org/10.1126/science.1116480

[19] Hussain, I., Hussain, A., Alajmi, M. F., Rehman, M. T., and Amir, S. (2021). Impact of repurposed drugs on the symptomatic COVID-19 patients. Journal of Infection and Public Health. 14(1): 24–38. https://doi.org/10.1016/j.jiph.2020.11.009.

[20] Cao, B., Wang, Y., Wen, D., Liu, W., Wang, J., Fan, G., Ruan, L., et al. (2020). A trial of lopinavir-ritonavir in adults hospitalized with severe COVID-19. N Engl J Med. 382(19):1787–1799. https://doi.org/10.1056/nejmoa2001282

[21] Fan, C., Li, K., Ding, Y., Lu, W.L., Wang, J. (2021). ACE2 expression in kidney and testis may cause kidney and testis damage after 2019-nCoV infection. Front Med (Lausanne), 7:563893. https://doi.org/10.3389/fmed.2020.563893

[22] Kim, S., Chen, J., Cheng, T., Gindulyte, A., He, J., He, S., Li, Q., Shoemaker, B. A., Thiessen, P. A., Yu, B., Zaslavsky, L., Zhang, J., Bolton, E.E. (2023). PubChem 2023 update. Nucleic Acids Research, Vol. 51, Database issue D1373–D1380. https://doi.org/10.1093/nar/gkac956

[23] Bendjeddou, A., Abbaz, T., Gouasmia, A., Villemin, D. (2016). Quantum Chemical Studies on Molecular Structure and Reactivity Descriptors of some p-Nitrophenyl Tetrathiafulvalenes by Density Functional Theory (DFT). Acta. Chim. Pharm. Indica, 6(2): 32-44.

[24] Bag, A. (2021). DFT based Computational Methodology of IC50 Prediction. Curr Comput Aided Drug Des., 17(2):244-253. https://doi.org/10.2174/1573409916666200219115112

[25] Becke, A. D. (2018). Density-functional exchange-energy approximation with correct asymptotic behavior. Phys Rev A Gen Phys. 38(6):3098-3100. https://doi.org/10.1103/physreva.38.3098

[26] Lee, C., Yang, W., Parr, R. G. (1988). Development of the Colle-Salvetti correlation-energy formula into a functional of the electron density. Phys. Rev. 37: 785-789. https://doi.org/10.1103/physrevb.37.785

[27] Parr, R. G., Pearson, R. G. (1983). Absolute hardness: companion parameter to absolute electronegativity. J. Am. Chem. Soc. 105: 7512-7516. https://doi.org/10.1021/ja00364a005

[28] Nolasco, M. M., Araujo, C. F., Vaz, P. D., Amado, A. M., Ribeiro-Claro, P. (2020). Vibrational Dynamics of Crystalline 4-Phenylbenzaldehyde from INS Spectra and Periodic DFT Calculations. Molecules, 25(6):1374. https://doi.org/10.3390/molecules25061374

[29] Bag, A., Ghorai, P. K. (2015). Computational investigation of the ligand field effect to improve the photoacoustic properties of organometallic carbonyl clusters. RSC Adv. 5: 31575- 31583. https://doi.org/10.1039/C5RA01757B

[30] Marschallinger, J., Scha¨ffner, I., Klein, B., Gelfert, R., Rivera, F. J., et al. (2015). Structural and functional rejuvenation of the aged brain by an approved anti-asthmatic drug. Nature Communications 6:8466. https://doi.org/10.1038/ncomms9466

[31] Novakova, I., Subileau, E-A., Toegel, S., Gruber, D., Lachmann, B., Urban, E., Chesne, C., Noe, C. R., Neuhaus, W. (2014). Transport Rankings of Non-Steroidal Anti-inflammatory Drugs across Blood-Brain Barrier In Vitro Models. PLoS ONE 9(1): e86806. https://doi.org/10.1371%2Fjournal.pone.0086806

[32] Kumar, S., Singh, B., Kumar, P., Kumar, P.V., Agnihotri, G., Khan, S., Beuria, T.K., Syed, G.H., Dixit, A. (2021) Identification of Multipotent Drugs for COVID-19 Therapeutics with The Evaluation of Their SARS-CoV-2 Inhibitory Activity. Computational and Structural Biotech. Journal. 19: 1998-2017. https://doi.org/10.1016/j.csbj.2021.04.014.

[33] Hosseini, M., Chen, W., Wang, C. (2020). Computational Molecular Docking and Virtual Screening Revealed Promising SARS-CoV-2 Drugs. https://doi.org/10.26434/chemrxiv.12237995.v1

[34] Cao Y, Deng Q, and Dai S. (2020) Remdesivir for severe acute respiratory syndrome coronavirus 2 causing COVID-19: An evaluation of the evidence. Travel Med Infect. Dis: 10:1647, http://dx.doi.org/10.1016/j.tmaid.2020.101647.

[35] Schooley, R.T., Carlin, A.F., Beadle, J.R., Valiaeva, N., Zhang, X. Q., et al. (2021). Rethinking remdesivir: synthesis, antiviral activity and pharmacokinetics of oral lipid prodrugs. Antimicrob Agents Chemother., 65(10): e0115521. https://doi.org/10.1128/aac.01155-21

[36] Cao, Z., Gao, W., Bao, H., Feng, H., Mei, S., Chen, P., et al. (2023). VV116 versus nirmatrelvir-ritonavir for oral treatment of COVID-19. N Engl J Med. 388(5): 406–417. https://doi.org/10.1056/nejmoa2208822

[37] Gordon, C.J., Tchesnokov, E.P., Feng, J. Y., Porter, D.P., Götte, M. (2020). The Antiviral Compound Remdesivir Potently Inhibits RNA-dependent RNA polymerase from Middle East Respiratory Syndrome Coronavirus. J Biol Chem. 295, 4773-4779. https://doi.org/10.1074/jbc.ac120.013056

[38] Sheahan, T. P., Sims, A.C., Leist, S.R., Schafer, A., Won, J., Brown, A.J., et al. (2020). Comparative Therapeutic Efficacy of Remdesivir and Combination Lopinavir, Ritonavir, and Interferon beta against MERS-CoV. Nat Commun., 11(1):222. https://doi.org/10.1038/s41467-019-13940-6

[39] Grein, J., Ohmagari, N., Shin, D., Diaz, G., Asperges, E., Castagna, A., et al. (2020). Compassionate Use of Remdesivir for Patients with Severe Covid-19. N. Engl. J. Med. 382:2327-36. https://doi.org/10.1056/nejmoa2007016

[40] Sheahan, T.P., Sims, C., Zhou, S., Graham, R.L., Pruijssers, A.J., et al. (2020). An orally bioavailable broad-spectrum antiviral inhibits SARS-CoV-2 in human airway epithelial cell cultures and multiple coronaviruses in mice. Sci Transl Med. 12(541): eabb5883. https://doi.org/10.1126/scitranslmed.abb5883